Monthly Notices
of the
ROYAL ASTRONOMICAL SOCIETY

MNRAS **467,** 1608–1613 (2017)
Advance Access publication 2017 January 22

doi:10.1093/mnras/stx190

# Assessment of different sunspot number series using the cosmogenic isotope $^{44}$Ti in meteorites

Eleanna Asvestari,[1] Ilya G. Usoskin,[1,2]★ Gennady A. Kovaltsov,[3] Mathew J. Owens,[4]★ Natalie A. Krivova,[5] Sara Rubinetti[6,7] and Carla Taricco[6,7]

[1]*Space Climate Research Unit, University of Oulu, FIN-90017 Oulu, Finland*
[2]*Sodankylä Geophysical Observatory (Oulu unit), University of Oulu, FIN-90017 Oulu, Finland*
[3]*Ioffe Physical-Technical Institute, St. Petersburg, RU-194021, Russia*
[4]*Department of Meteorology, University of Reading, Earley Gate, Reading RG6 6BB, UK*
[5]*Max-Planck-Institut für Sonnensystemforschung, Justus-von-Liebig-Weg 3, D-37077 Göttingen, Germany*
[6]*Dipartimento di Fisica, Via P.Giuria 1, Università di Torino, I-10125 Torino, Italy*
[7]*Istituto Nazionale di Astrofisica, Osservatorio Astrofisico di Torino, Strada Osservatorio 20, I-10025 Pino Torinese, Italy*

Accepted 2017 January 19. Received 2017 January 19; in original form 2016 November 10

## ABSTRACT

Many sunspot number series exist suggesting different levels of solar activity during the past centuries. Their reliability can be assessed only by comparing them with alternative indirect proxies. We test different sunspot number series against the updated record of cosmogenic radionuclide $^{44}$Ti measured in meteorites. Two bounding scenarios of solar activity changes have been considered: the HH-scenario (based on the series by Svalgaard and Schatten), in particular, predicting moderate activity during the Maunder minimum, and the LL-scenario (based on the $R_G$ series by Lockwood et al.) predicting moderate activity for the 18th–19th centuries and the very low activity level for the Maunder minimum. For each scenario, the magnetic open solar flux, the heliospheric modulation potential and the expected production of $^{44}$Ti were computed. The calculated production rates were compared with the corresponding measurements of $^{44}$Ti activity in stony meteorites fallen since 1766. The analysis reveals that the LL-scenario is fully consistent with the measured $^{44}$Ti data, in particular, recovering the observed secular trend between the 17th century and the Modern grand maximum. On the contrary, the HH-scenario appears significantly inconsistent with the data, mostly due to the moderate level of activity during the Maunder minimum. It is concluded that the HH-scenario sunspot number reconstruction significantly overestimates solar activity prior to the mid-18th century, especially during the Maunder minimum. The exact level of solar activity after 1750 cannot be distinguished with this method, since both H- and L- scenarios appear statistically consistent with the data.

**Key words:** sunspots.

## 1 INTRODUCTION

The sunspot number (SN) record is the longest instrumental scientific series forming a benchmark for numerous studies of solar and stellar variability. Easy times of a single 'gold standard' SN series, used by everyone, are over. At present, there are a handful of independent SN reconstructions, all differing in their assessments of the level of solar activity in the past (e.g. Hoyt & Schatten 1998; Clette et al. 2007; Clette et al. 2014; Lockwood, Owens & Barnard 2014b; Svalgaard & Schatten 2016; Usoskin et al. 2016a; Friedli 2017). These SN series are based on a significant number of fragmentary observations by individual observers, each subject to different processing techniques. An essential part of any SN series is compilation and intercalibration of records by individual observers, which can be done in different ways. All the various series can be divided into two categories according to their construction procedure: (1) SN that count both the weighted number of sunspot groups and individual spots (Wolf sunspot numbers, WSN, and International sunspot numbers, ISN, are the examples); and (2) group sunspot numbers, GSN, that only count sunspot groups. While WSN/ISN are still traditionally considered as an index of solar activity, the GSN offer a more robust measure and, in addition, allow access to full raw data (see more details in Usoskin 2013). Reconstructions also differ in the method of calibration of individual observers to some standard observational conditions.

In the wake of different methods, the reconstructions show different levels of solar activity in the past. While nearly all SN series

★ E-mail: ilya.usoskin@oulu.fi (IGU); m.j.owens@reading.ac.uk (MJO)

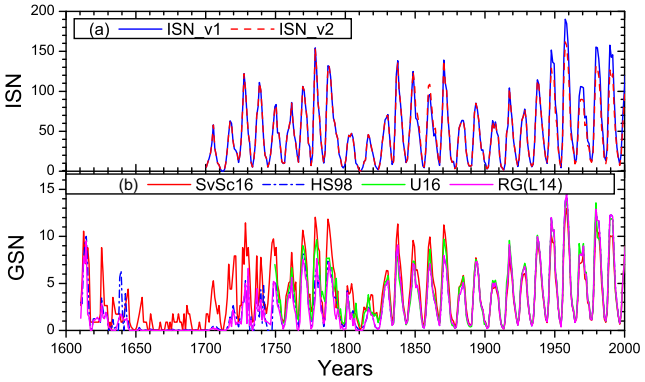


**Figure 1.** Temporal variation of the yearly means of the different reconstructions of SN series: Panel (a): ISN versions 1 (ISN_v1) and 2 (ISN_v2). Panel (b): the GSN by SvSc16 (red curve), by HS98 (blue dot–dashed curve), by Usoskin et al. (2016a) (U16, green curve) and by L14b (magenta curve).

agree over the 20th century, thanks to the high quality and professional style of solar observations, the levels of sunspot activity during and before the 19th century differ significantly among the series, with the difference being critical before 1750. Roughly, the SN reconstructions can be divided into 'high' and 'low'. The high reconstructions (Svalgaard & Schatten 2016) suggest that the level of sunspot activity, as compared to that in the late 20th century, was high during the 19th and 18th century, and moderate but not low during the Maunder minimum in the second half of the 17th century. The low reconstructions (e.g. Lockwood et al. 2014b) imply that the level of activity was significantly lower during the 18th–19th centuries than during the Grand maximum in the 20th century (Solanki et al. 2004), and that the sunspot activity was very low during the Maunder minimum. A series by Usoskin et al. (2016a) is moderate and lies between the high and low ones.

Examples of different series are shown in Fig. 1: high series as represented by the GSN reconstruction (Svalgaard & Schatten 2016 – SvSc16 henceforth), low series by GSN series of $R_C$ (Lockwood et al. 2014b – henceforth L14) and moderate GSN series by Usoskin et al. (2016a, henceforth Us16). Henceforth, we consider three scenarios of the evolution of solar activity over the last centuries:

(i) The HH-scenario based on the SvSc16 series, which yields the highest, among all considered reconstructions, level of activity both before 1750 (in particular, a moderate activity level during the Maunder minimum) and over 1750–1950;

(ii) The LL-scenario based on the $R_G$ series by L14, which yields the conventionally low level of solar activity during the Maunder minimum and the lowest among all reconstructions level during 1750–1950;

(iii) Additionally, we consider an LH-scenario that is a combination of the L-scenario (low Maunder minimum) before 1750 and the H-scenario (high activity) after 1750.

Because of the benchmark status for long-term solar variability, it is crucially important to assess fidelity and reliability of different SN series. However, SN series cannot be internally verified, and no self-consistency checks are available beyond some non-strict empirical relations between the length and the amplitude of solar cycle (Waldmeier 1935; Hathaway 2015) or between the number of sunspots and groups (Friedli 2017). Accordingly, it is hardly possible to assess the reliability of different series from the sunspot data alone. Assessment can be performed only using indirect proxies, such as geomagnetic, heliospheric or cosmogenic. Several such efforts have been made but turned inconclusive and mutually controversial (Lockwood et al. 2016a,c; Owens et al. 2016a; Svalgaard 2016). Moreover, Svalgaard (2016), using data on the diurnal variability of the geomagnetic field, proposed that 'the Relative Sunspot Number as currently defined is beginning to no longer be a faithful representation of solar magnetic activity', implying a discrepancy between geomagnetic and sunspot records. Cosmogenic isotopes, mostly $^{14}$C and $^{10}$Be, measured in natural terrestrial archives, provide a quantitative proxy for solar activity (Beer, McCracken & von Steiger 2012; Usoskin 2013). However, this method can be hardly applied for the 20th century because of the anthropogenic effects (fossil fuel burning, land-use changes and atmospheric nuclear bomb tests) and climate changes that affect the cosmogenic isotope transport and deposition. As a result, applications of the cosmogenic isotope data to assess quality of different SN reconstructions were also inconclusive and contradictory; Muscheler et al. (2016) found, using an ad hoc normalization, that the high SN series agree with the cosmogenic record, but they did not analyse other sunspot series; Usoskin et al. (2015) concluded that while low SN series agree with the cosmogenic $^{14}$C data, the high series do not; Owens et al. (2016b) suggested that all SN series agree more or less with cosmogenic $^{10}$Be data, within the uncertainties. Probably, such ambiguity of the results is related to the fact that changes in the solar activity are governed by the 11-yr cycle that is, of course, synchronous in all the SN reconstructions, with the only difference being in the amplitude.

Thus, the level of solar activity in different SN reconstructions remains poorly constrained before the mid-18th century, but relatively well known since the late 19th century. Here we propose a new test of the different SN reconstructions against the activity of cosmogenic isotope $^{44}$Ti measured in fallen meteorites since 1766 (Taricco et al. 2006; Usoskin et al. 2006). This quantitative proxy is free of any terrestrial or anthropogenic influence, since the isotope is produced in space during irradiation of the meteorite's body by cosmic-ray protons (>70 MeV), as a result of spallation of Fe and Ni. Moreover, due to its long half-life, it is insensitive to the 'short-term' (11-yr cycle) variability but very sensitive to the centennial and multicentennial variations of solar activity. As a drawback, this method does not allow us to assess mid-term (decades to a century) variability.

We do not discuss here details of the SN series constructions but make a blind test of their consistency with the cosmic-ray flux in the past. Using different SN series, we first computed the magnetic open solar flux (OSF), as described in Section 3.1. From the OSF series, we then calculated the heliospheric modulation potential (Section 3.2) using a semi-empirical model by Asvestari & Usoskin (2016), and subsequently, from this modulation potential, we calculate the production rate of the cosmogenic isotope using the $^{44}$Ti production model (as discussed in Section 3.3). The results are compared with the measured $^{44}$Ti activity. We summarize our conclusion in Section 4.

## 2 THE SN SERIES

The first effort to conflate the SN observations into a single series was made by Rudolf Wolf in the mid-19th century. In an attempt to create a homogeneous series, he used only the primary observer for each day (or secondary, etc., if the primary one was unavailable), overlooking a large fraction of daily observations. Following nearly the same technique, the WSN series continued to be constructed until 1980 at the Zürich Observatory (Zürich SN, $R_z$), and from 1981 onwards by the Royal Observatory of Belgium (ROB), which founded the Sunspot Index Data Center. While adopting the Zürich

algorithm to construct the SN, ROB introduced a new method to derive the daily SN (ISN) using multiple individual observations for each day after 1980. The earlier (before 1980) part of the ISN record is based on the WSN series.

Although Wolf extended his series back to 1749, he used interpolation or indirect data to fill the data gaps, which introduced additional uncertainties. Another disadvantage of this series is that when Wolfer took it over from Wolf, he continued its compilation following different sunspot selection criteria, and instead of revisiting the entire reconstructed series by Wolf, he only introduced a scaling factor based on a comparison of his own and Wolf's observations over the period of the overlap (Clette et al. 2014). Furthermore, Waldmeier also changed the method of constructing the SN series introducing a weighting factor for each individual sunspot based on their size. However, no full revision of the entire WSN series can be done, with only a scaling correction introduced (Clette et al. 2014). Thus, the way this series was constructed makes it hardly verifiable and not always consistent. Nowadays, two versions of the ISN exist (version 1 and 2) provided by the WDC-SILSO, ROB.

Fig. 1(a) compares the two SN series ISN_v1 and ISN_v2 (http://sidc.be/silso/datafiles, responsible person F. Clette), where the latter is multiplied with the constant factor of 0.6 to bring it to the same level as the former (Clette et al. 2014). The two curves are very close to each other except for two periods: the ISN_v2 is higher than ISN_v1 around 1860s because of the Wolf correction, and lower than that after 1940 because of the correction for Waldmeier discontinuity.

Hoyt & Schatten (1998, hereafter HS98) introduced the GSN and produced the original GSN series by reconsidering all the individual archives and taking into account additional sunspot observations, which Wolf was not aware of or did not include in his reconstruction. This also allowed the authors to extend the series further back in time. Going back to 1610, this series includes the very interesting period of the Maunder Minimum (1645–1715). By focusing on the sunspot groups, the GSN surpasses the issue of the visibility of small spots since a group of several small spots would appear as one blurred spot for an observer with a poor telescope. However, this introduces another potential uncertainty of grouping individual spots that could be done by early-time observers differently from how we would do it nowadays (Clette et al. 2014). This uncertainty enters both GSN (directly) and WSN/ISN series (since the number of groups composes 50–90 per cent of the WSN/ISN values). Since all the original data composing the GSN are archived in a digital format (HS98), the series is fully transparent and verifiable. Despite all the advantages, this series is not free of uncertainties either, leaving room for improvement. Corrections for some apparent inhomogeneities in the HS98 GSN series have been recently proposed by L14b leading to the $R_G$ L14 series. In particular, a daisy-chain normalization of different observers to the reference observational conditions may be partly incorrect (Clette et al. 2014; Cliver & Ling 2016) and needs to be revisited. Since the GSN series contains the full and continuously updated (e.g. Vaquero & Vázquez 2009; Vaquero et al. 2011, 2016) data base of raw data, it is possible to revisit the entire series, as was done recently by SvSc16 or Usoskin et al. (2016a).

All previous SN series, including also the recent ones, SvSc16 and L14, were based on the linear scaling between different observers. However, as shown in recent studies (Lockwood et al. 2016b; Usoskin, Kovaltsov & Chatzistergos 2016b; Usoskin et al. 2016a), the method of linear scaling correction (the so-called *k*-factors) used to construct all the earlier series may lead to possible distortions of the final series as seen, for example, in a significant difference

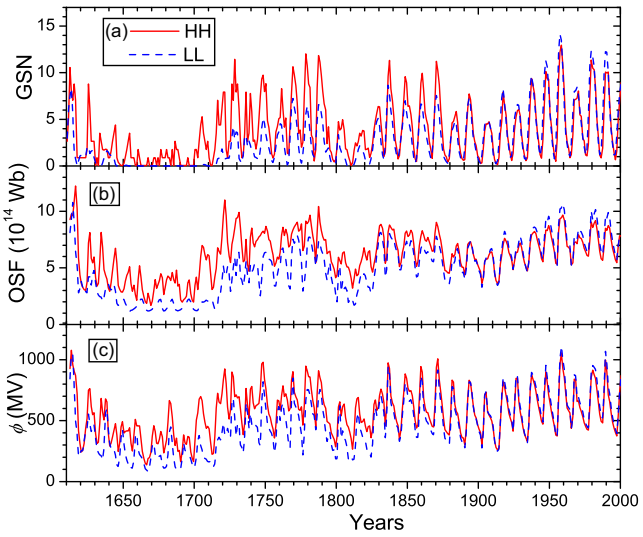


**Figure 2.** Time variability of the considered HH- and LL- scenarios, as indicated in the legend. The LH-scenario is a composition of the LL-scenario before 1750 and the HH-scenario after that. Panel (a): number of sunspot groups; Panel (b): OSF; Panel (c): the modulation potential $\phi$. Annual values are shown. Error bars are not shown for clarity.

between the L14 and SvSc16 series based on the same data set and similar *k*-factor approaches. Only a few recent reconstructions of the SN series (Usoskin et al. 2016a; Friedli 2017) are based on direct statistical methods without the daisy-chaining calibration via linear scaling *k*-factors.

Fig. 1(b) compares some GSN series, representing the high, low and intermediate series. The 'classical' GSN series, HS98 (Hoyt & Schatten 1998), was taken from SILSO (http://www.sidc.be/silso/groupnumberv3, responsible person F. Clette). The new GSN series, SvSc16, was constructed by Svalgaard & Schatten (2016), based on the HS98 data base using a modified *k*-factor ('backbone') calibration. Another GSN series $R_G$, by L14, corrected for some proposed errors, was constructed by L14b. The Us16 series (Usoskin et al. 2016a) is another new GSN series, also based on the HS98 data base but applying an independent, daisy-chain-free calibration based on the statistics of active day fraction.

In the following, we will consider the HH-, LH- and LL- scenarios (as described in Section 1) of solar activity evolution. The HH- and LL-scenarios are shown in Fig. 2(a), while the LH-scenario is a composite of the LL-scenario before 1750 and the HH-scenario after 1750.

## 3 MODELING THE $^{44}$TI RECORDS

Here we model the production of $^{44}$Ti in a standard stony meteorite, following the method described in Usoskin et al. (2006), and compare it with the measured activity of $^{44}$Ti in fallen meteorites.

### 3.1 The magnetic OSF

The three solar activity scenarios mentioned above were employed to compute the OSF using the model proposed by Owens & Lockwood (2012) and L14b and updated by Owens et al. (2016a). In brief, the OSF is modelled as a continuity equation (Solanki, Schüssler & Fligge 2000), with the source term, *S*, set by an empirical relation to SN using the data for the recent decades. The loss term, *L*, varies with the heliospheric current sheet inclination,

which is assumed to be invariant between solar cycles (Asvestari & Usoskin 2016). The magnitude of $L$ was derived using comparison with an OSF series, determined empirically from geomagnetic data for 1845–2013 (Lockwood et al. 2014a). Uncertainties in the sunspot-based OSF estimate were also obtained using the comparison to the geomagnetic record, according to Lockwood & Owens (2014). This model also depicts excellent agreement with direct OSF measurements during the last decades and the geomagnetic data since 1845 (Owens et al. 2016a), suggesting that the model uncertainties are small. Fig. 2(b) shows the OSF reconstructions for the HH- and LL-scenarios. They agree relatively well with each other for the period after 1830 but exhibit a notable difference before that. The difference is particularly large during the Maunder Minimum, MM, 1645–1715, when the reconstruction based on the HH-scenario exhibits a much higher level of solar activity compared to the LL-scenario. Since one and the same OSF model was used for all the scenarios, the difference in the computed OSF is caused by the difference in the SN series before the 19th century.

### 3.2 The heliospheric modulation potential

The spectrum of Galactic cosmic rays (GCR) near Earth can be described by the force-field parametrization using a single parameter, called the modulation potential (Gleeson & Axford 1968; Castagnoli & Lal 1980; Usoskin et al. 2005), which depends on the level of solar magnetic activity. One of the main heliospheric parameters, affecting the modulation potential, $\phi$, is the OSF. Here we use a semi-empirical heliospheric modulation model (Asvestari & Usoskin 2016), which uses the OSF, the tilt angle of the heliospheric current sheet and the polarity of the heliospheric magnetic field to compute the modulation potential. Changes in the solar wind velocity and density are not considered in the model since their net relation with the global cosmic-ray modulation is insignificant (Belov 2000; Alanko-Huotari et al. 2006; Sabbah & Rybansky 2006). We adopt this model to estimate the modulation potential from the OSF reconstruction discussed above, considering the solar cycle length and phasing as defined by the solar maxima and minima listed in ftp://ftp.ngdc.noaa.gov/STP/space-weather/solar-data/solar-indices/sunspot-numbers/cycle-data/table_cycle-dates_maximum-minimum.txt. The error propagation was made straightforwardly including also uncertainties of the applied model.

The exact value of the modulation potential is not important since it can be defined only relatively, depending on the primary assumption on the local interstellar spectrum (LIS) so that the same GCR spectrum near Earth can be parametrized by different values of $\phi$ for different LIS assumptions (Usoskin et al. 2005; Herbst et al. 2010). However, once the LIS is fixed, the value of $\phi$ unambiguously determines the GCR energy spectrum. Here we use the modulation potential based on the LIS by Burger, Potgieter & Heber (2000), and all the values of the modulation potential are referred to this LIS. We have checked that the exact choice of reference LIS does not affect our result.

The modulation potential series, derived here, are shown in Fig. 2(c). The HH-scenario yields systematically stronger GCR modulation than the LL-scenario prior to 1830. This is particularly pronounced around the MM.

### 3.3 $^{44}$Ti in meteorites: measured and computed activity

The activity of $^{44}$Ti was measured in 20 stony meteorites (ordinary chondrites) that were selected based on size and date of fall to cover the interval 1766–2001 (Taricco et al. 2006, 2008, 2016).

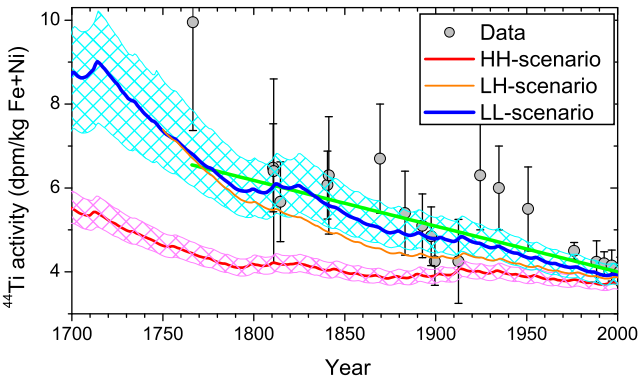


**Figure 3.** Time profile of the $^{44}$Ti activity in units of disintegrations per minute per kg of iron and nickel in a meteorite. Grey circles with error bars denote the measurements (Taricco et al. 2006, 2008, 2016). The thick green line represents the best linear fit (using the weighted least-squares method) to the $^{44}$Ti data. The red, blue and orange curves depict the computed activity for the HH-, LL- and LH-scenarios, respectively (see the text). Hatched areas correspond to $1\sigma$ modelling uncertainties including also those of the $^{44}$Ti production. Uncertainties of the LH-scenario are not shown for clarity.

The very low activity of this isotope, mainly related to the low-production cross-sections and to the decay since the time of fall, was revealed using highly selective gamma-ray Ge-Na I (Tl) spectrometers (Taricco et al. 2006; Taricco et al. 2007) located at the underground Laboratory of Monte dei Cappuccini (OATo-INAF) in Torino, Italy. Fig. 3 shows the measured activity (grey dots), corrected for shielding depth within the parent meteoroids and for target element composition (see the details in Taricco et al. 2006). The error bars represent the statistical errors of measurements ($1\sigma$). We note that this data set is updated, including more data points, with respect to earlier studies (Taricco et al. 2006; Usoskin et al. 2006; Usoskin et al. 2015). We used this data set to test different SN scenarios by applying the method developed by Usoskin et al. (2006). Here we considered only long sunspot series covering the Maunder minimum, since other series (US16, ISN_v1 and ISN_v2) are too short to be directly applied to the $^{44}$Ti without an extension for at least one to two lifetimes backward in time.

First, we used the OSF and the modulation potential $\phi$ since 1610 for different scenarios, as described in Sections 3.1 and 3.2, to compute the $^{44}$Ti production $Q$ in a meteorite. This was done using a production model by Michel & Neumann (1998), as described in great detail by Usoskin et al. (2006). To obtain a reasonable equilibrium level of $^{44}$Ti in 1610, when the SN series start, we used the reconstruction of $\phi$ for 10 lifetimes before 1610, viz. since 750 AD, based on $^{14}$C data (Usoskin et al. 2014). We note that the exact history of $^{44}$Ti before 1610 is not important since the first meteorite we use fell in 1766, viz. two lifetimes after that. Next, we calculated the expected $^{44}$Ti activity $A_i$ in a meteorite fallen in the year $i$ as the balance between production and decay:

$$A(t) = \frac{1}{\tau}\int_{-\infty}^{t} Q(t') \times \exp\left(\frac{t-t'}{\tau}\right) \times \mathrm{d}t', \qquad (1)$$

where the first and the second terms describe the production and decay, respectively, $\tau$ is the mean lifetime of the isotope ($85.4 \pm 0.9$ yr as used in Usoskin et al. 2006 – see Taricco et al. 2006 for a review of $^{44}$Ti half-life measurements) and $Q_i$ is the production term. The value of $A_i$ gives the activity of $^{44}$Ti expected to be in a meteorite fallen in year $i$. The computed activity for each scenario is shown in Fig. 3 (solid curves) for 1700–2001, with the model uncertainties indicated by the hatched areas, compared to the measured (circles)

activities. The shown uncertainties consist of both the uncertainties of the modulation potential (as shown in Fig. 2c) and the uncertainties of the $^{44}$Ti modelling (Usoskin et al. 2006).

As a quantitative measure of the comparison between the measured and predicted values of $A$, we used the $\chi^2(20)$-value with 20 degrees of freedom. The uncertainties used to calculate $\chi^2$ include both the measurement error bars and uncertainties of the computations, as shown in Fig. 3. Both LL- and LH-scenarios give low $\chi^2(20)$ values of 10.7 and 19.4, respectively, which implies their full consistency with the observations (the $p$-values are 0.95 and 0.50, respectively). Thus, even though the LL-scenario yields a formally better agreement with the $^{44}$Ti data, we cannot distinguish here, with a statistical confidence, between high- and low-activity scenarios after 1750. In contrast, the curve based on the HH-scenario lies systematically apart from the measured activities, with $\chi^2(20) = 54.1$, suggesting that the hypothesis that it agrees with the data should be rejected with the very high significance of $6 \times 10^{-5}$. Thus, the moderate activity predicted by the HH-scenario around and during the Maunder minimum is inconsistent with the $^{44}$Ti data, likely because of the poor quality of sunspot data before 1749.

We note that all curves lie slightly but systematically below the data points. This suggests a possible weak underestimate of the $^{44}$Ti production by the model. This uncertainty is seen as a 5–10 per cent disagreement (being fully within the shown error bars) between the most recent meteorites and the model curves. If we introduce a free scaling parameter (thus reducing the number of degrees of freedom by one) to match the model curve to the level of the most recent meteorites (1990–2001), this does not alter the conclusion: The LL- and LH-scenarios remain fully consistent with the data ($p = 0.97$ and 0.95, respectively), while the hypothesis of the agreement between the HH-scenario and the data should be rejected at a significant level of 0.03.

We also note that the overall declining trend is the main feature of the $^{44}$Ti data (Taricco et al. 2006), which clearly suggests a gradual change in solar activity between the Maunder minimum and the modern time. The trend in the data is such that the $^{44}$Ti activity has dropped (as shown by the green line in Fig. 3), during the interval 1766–2001, by a factor of $1.61 \pm 0.2$, due to the increasing solar activity. We note that this ratio is free of any model uncertainties and thus may serve as a robust estimate of the centennial variability of solar activity. Over the same time interval (1766–2001), the LL- and LH-based scenarios yield a decline of factor of $1.67 \pm 0.15$ and $1.68 \pm 0.15$, respectively, in good agreement with the $^{44}$Ti data, within the $1\sigma$ uncertainties. On the contrary, the HH-scenario yields a much smaller trend, $1.12 \pm 0.06$, which is $2.4\sigma$ away from the observed ratio. The lack of a secular trend is a principal feature of the SvSc16 series (Clette et al. 2014), as reflected by the flatness of the red curve (HH-scenario) of Fig. 3, which disagrees with the measured trend irrespective of the possible model uncertainty.

Therefore, while the LL- and LH-scenarios appear consistent with the measurements of $^{44}$Ti in meteorites, the HH-based scenario is inconsistent with them implying systematically too low flux of cosmic rays (too high solar activity) between 1610 and roughly 1750, including the Maunder minimum. On the other hand, the exact level of solar activity after 1750 cannot be assessed with this method so that both H- and L-scenarios appear statistically consistent with the cosmogenic data.

## 4 CONCLUSIONS

In this work, we considered three scenarios of solar activity levels during the 17–20th centuries: (1) the upper bound HH-scenario, represented by the SvSc16 series, which predicts, in particular, a moderate level of activity during the Maunder minimum; (2) the lower bound LL-scenario, represented by the $R_G$ L14 series, which implies, in particular, a very low level of activity during the Maunder minimum; and (3) LH-scenario, which is a combination of the LL-scenario prior to 1750 and the HH-scenario after that. We have tested these scenarios against an updated data set of measurements of cosmogenic isotope $^{44}$Ti in 20 meteorites fallen after 1766. Series, not extending back to the Maunder minimum (ISN_v1, ISN_v2, Us16), cannot be tested here because of insufficient lengths. Moreover, while the LL-scenario exhibits a formally better agreement with the $^{44}$Ti data than LH-scenario (see Fig. 3), the difference is not statistically significant, and we cannot judge here about the exact level of activity after 1750.

For each SN scenario, we first reconstructed the OSF as described in Section 3.1, then the modulation potential (Section 3.2), and finally the $^{44}$Ti production in meteorites (Section 3.3). We quantify the agreement between the SN scenarios and the measured $^{44}$Ti data via the $\chi^2$-statistics.

We conclude that both the LL- and LH-scenarios are fully consistent with the $^{44}$Ti data and reproduce the long-term trend that is the dominant feature of the $^{44}$Ti data (Taricco et al. 2006). In contrast, the HH-scenario significantly overestimates solar activity prior to the mid-18th century and especially during the periods of Maunder Minimum (1645–1715). In particular, the HH-scenario does not reproduce the long-term trend.

As the final note, we want to stress that this test is only indirectly based on proxy data and models with all their possible uncertainties. The results presented here make some indications of the consistency but ought not to be used as a basis for correction of one or the other SN series since the discrepancy between the SN and cosmic-ray variability may be real, especially for the times of Grand minima and maxima of solar activity. This leaves room for further improvements in the method.

## ACKNOWLEDGEMENTS

Leif Svalgaard is acknowledged for thorough reviewing of the manuscript. We thank Robert H. Cameron for useful discussion. Contributions of E. Asvestari, I.G. Usoskin and G.A. Kovaltsov were done in the framework of the ReSoLVE Centre of Excellence (Academy of Finland, project no. 272157). M. Owens is funded by the UK Science and Technology Facilities Council (STFC) consolidated grant number ST/M000885/1. Part of this work was supported by the COST Action ES1005 'Toward a more complete assessment of the impact of solar variability on the Earth's climate'.

## REFERENCES

Alanko-Huotari K., Mursula K., Usoskin I. G., Kovaltsov G. A., 2006, Sol. Phys., 238, 391
Asvestari E., Usoskin I. G., 2016, J. Space Weather Space Clim., 6, A15
Beer J., McCracken K., von Steiger R., 2012, Cosmogenic Radionuclides: Theory and Applications in the Terrestrial and Space Environments. Springer-Verlag, Berlin Heidelberg
Belov A., 2000, Space Sci. Rev., 93, 79
Burger R., Potgieter M., Heber B., 2000, J. Geophys. Res., 105, 27447
Castagnoli G., Lal D., 1980, Radiocarbon, 22, 133
Clette F., Berghmans D., Vanlommel P., Van der Linden R. A. M., Koeckelenbergh A., Wauters L., 2007, Adv. Space Res., 40, 919
Clette F., Svalgaard L., Vaquero J. M., Cliver E. W., 2014, Space Sci. Rev., 186, 35
Cliver E. W., Ling A. G., 2016, Sol. Phys., 291, 2763

Friedli T., 2017, Sol. Phys., in press
Gleeson L., Axford W., 1968, ApJ, 154, 1011
Hathaway D. H., 2015, Living Rev. Sol. Phys., 12, 4
Herbst K., Kopp A., Heber B., Steinhilber F., Fichtner H., Scherer K., Matthiä D., 2010, J. Geophys. Res., 115, D00I20
Hoyt D. V., Schatten K. H., 1998, Sol. Phys., 181, 491 (HS98)
Lockwood M., Owens M. J., 2014, J. Geophys. Res.: Space Phys., 119, 5193
Lockwood M., Nevanlinna H., Barnard L., Owens M. J., Harrison R. G., Rouillard A. P., Scott C. J., 2014a, Ann. Geophys., 32, 383
Lockwood M., Owens M. J., Barnard L., 2014b, J. Geophys. Res.: Space Phys., 119, 5172 (L14b)
Lockwood M., Owens M. J., Barnard L., Scott C. J., Usoskin I. G., Nevanlinna H., 2016a, Sol. Phys., 291, 2811
Lockwood M., Owens M. J., Barnard L., Usoskin I. G., 2016b, Sol. Phys., 291, 2829
Lockwood M., Owens M. J., Barnard L., Usoskin I. G., 2016c, ApJ, 824, 54
Michel R., Neumann S., 1998, Earth. Planet. Sci., 107, 441
Muscheler R., Adolphi F., Herbst K., Nilsson A., 2016, Sol. Phys., 291, 3025
Owens M. J., Lockwood M., 2012, J. Geophys. Res., 117, A04102
Owens M. J. et al., 2016a, J. Geophys. Res.: Space Phys., 121, 6048
Owens M. J. et al., 2016b, J. Geophys. Res.: Space Phys., 121, 6064
Sabbah I., Rybansky M., 2006, J. Geophys. Res., 111, A01105
Solanki S. K., Schüssler M., Fligge M., 2000, Nature, 408, 445
Solanki S., Usoskin I., Kromer B., Schüssler M., Beer J., 2004, Nature, 431, 1084
Svalgaard L., 2016, Sol. Phys., 291, 2981
Svalgaard L., Schatten K. H., 2016, Sol. Phys., 291, 2653 (SvSc16)
Taricco C., Bhandari N., Cane D., Colombetti P., Verma N., 2006, J. Geophys. Res., 111, A08102
Taricco C., Bhandari N., Colombetti P., Verma N., Vivaldo G., 2007, Nucl. Inst. Meth. Phys. Res. A, 572, 241
Taricco C., Bhandari N., Colombetti P., Verma N., 2008, Adv. Space Res., 41, 275
Taricco C., Sinha N., Bhandari N., Colombetti P., Mancuso S., Rubinetti S., Barghini D., 2016, Ap&SS, 361, 338
Usoskin I. G., 2013, Living Rev. Solar Phys., 10, 1
Usoskin I. G., Alanko-Huotari K., Kovaltsov G. A., Mursula K., 2005, J. Geophys. Res., 110, A12108
Usoskin I. G., Solanki S. K., Taricco C., Bhandari N., Kovaltsov G. A., 2006, A&A, 457, L25
Usoskin I. G. et al., 2014, A&A, 562, L10
Usoskin I. G. et al., 2015, A&A, 581, A95
Usoskin I. G., Kovaltsov G. A., Lockwood M., Mursula K., Owens M., Solanki S. K., 2016a, Sol. Phys., 291, 2685
Usoskin I. G., Kovaltsov G. A., Chatzistergos T., 2016b, Sol. Phys., 291, 3793
Vaquero J. M., Vázquez M., 2009, The Sun Recorded Through History: Scientific Data Extracted from Historical Documents. Springer-Verlag, Berlin
Vaquero J. M., Gallego M. C., Usoskin I. G., Kovaltsov G. A., 2011, ApJ, 731, L24
Vaquero J. M. et al., 2016, Sol. Phys., 291, 3061
Waldmeier M., 1935, Astron. Mitt. Z., 6, 105

This paper has been typeset from a TEX/LATEX file prepared by the author.